

# Evaluating non articular causes of shoulder pain: A prospective study to determine the diagnostic accuracy of Ultrasound in reference to conventional MRI

Thesis

Submitted for Partial Fulfillment of Master Degree in Radio diagnosis

Presented by

Sarah Wagdy Shaker Mohammed

(M.B.B.CH)

Supervised By
Prof. Dr. Hanan Mahmoud Arafa

Professor of Radio Diagnosis
Faculty of Medicine - Ain Shams University

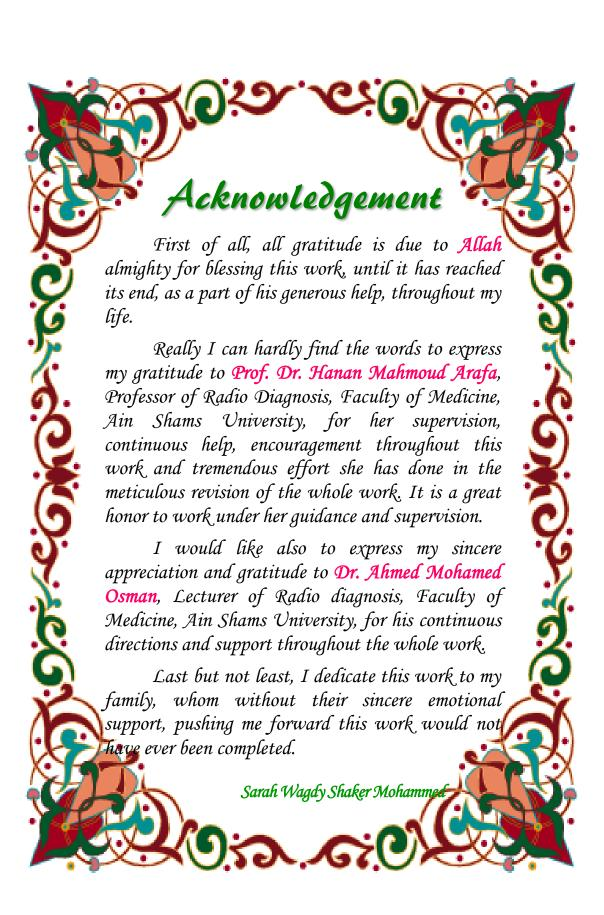
#### **Dr. Ahmed Mohamed Osman**

Lecturer of Radio diagnosis
Faculty of Medicine - Ain Shams University

Faculty of Medicine Ain Shams University 2017

## **List of The Contents**

Pa	age
Acknowledgment	
List of Abbreviations i	ĺ
List of Tablesi	iii
List of Figures	iv
Introduction	1
Aim of the work	3
Review of literature.	4
MRI anatomy of shoulder joint	4
• Technique of the shoulder joint MRI	33
• US anatomy and technique	37
Ultrasound and MRI Assessment of Painful Shoulder	ler
Joint5	53
Materials and methods	77
Results. 8	84
Illustrative cases.	94
Discussion	117
Summary and conclusion. 1	126
References. 1	129
Arabic summary	



#### List of Abbreviations

AC : Acromioclavicular

ACJ : Acromioclavicular Joint CHL : Coracohumeral ligament

DM : Diabetes mellitusGT : Greater tuberosity

IGHL : Inferior gleno humeral ligament

LHB : Long head of bicepsLT : Lesser tuberosity

MGHL: Middle gleno-humeral ligament
MRI: Magnetic Resonance Imaging

OA : os acromiale

PMR : Polymyalgia rheumatica

Sc : Subscapularis

SGL : superior gleno-humeral ligament

SS : Supraspinatus

SST : Supraspinatus tendon

Sub : Subscapularis TE : Time to echo

TrTrapezius muscleTRTime to repetitionUSUltrasonographyUSGUltrasonography

## **List of Tables**

List of Tables				
Table	Title	Page		
1	Illustrates the US scanning protocol & patient positioning for each scan protocol	79		
2	Illustrates the parameters used for the MRI shoulder examination	82		
3	Demonstrates the distribution of age between selected patients	84		
4	Demonstrates the side of the affected shoulder & dominant shoulder joint distribution between the selected patients	85		
5	Demonstrates the risk factors for painful shoulder namely heavy use and trauma	85		
6	Demonstrates the incidence of night pain complaint as well as accompanying other joint pain in-between the selected patients	85		
7	Demonstrates incidence (a) and diagnostic validity (b) of supraspinatus tendinopathy and calcific tendinitis by U/S in reference to MRI	87		
8	Demonstrates prevalence (a) and diagnostic validity (b) of supraspinatus (SS) articular surface partial tear, bursal surface partial tear, interstitial partial tear and total cases with partial supraspinatus tears by U/S in reference to MRI	88		
9	Demonstrates prevalence (a) and diagnostic validity tests (b) of supraspinatus (SS) complete width complete full thickness tears, incomplete width full thickness tear and all cases with tears by U/S in reference to MRI	89		
10	Demonstrates prevalence (a) and diagnostic validity (b) of Acromioclavicular joint osteoarthritis and Sub acromial impingement by U/S in reference to MRI	90		

### List of Tables (Cont.)

Table	Title	Page
11	Demonstrates prevalence (a) and diagnostic validity test (b) of Sub acromial Subdeltoid bursitis, Shoulder joint effusion and long head of biceps (LHB) tenosynovitis by U/S in reference to MRI	91
12	Demonstrates prevalence (a) and diagnostic validity (b) of Subscapularis tear, Subscapularis tendinopathy and infraspinatus tendinopathy by U/S in reference to MRI	93

## **List of Figures**

Fig.	Title	Page
1	Osteology of bones forming shoulder joint	5
2	Various glenoid rim shapes and glenoid hypoplasia.	6
3	Tubercle of Assaki.	7
4	Normal humeral head versus Hill-Sachs	7
	lesion.	
5	Dorsally located humeral head cysts are shown on axial (left side) and parasagittal (right side) MR images.	8
6	Cysts(arrow) and contour irregularities in the lesser tuberosity associated with subscapularis tendon lesion	8
7	<b>A.</b> Volume-rendering multidetector computed tomography superior view shows the oblique course of the clavicle. <b>B.</b> Os acromiale.	10
8	Various acromion shapes.	11
9	Sublabral recess.	14
10	Buford complex.	15
11	Sagittal-oblique MR image of the shoulder shows middle glenohumeral ligament (arrow) and inferior glenohumeral ligament (arrowhead).	17
12	Sagittal T2-weighted MR image with fat saturation demonstrates prominent anterior band of the IGHL seen attaching high at the level of the superior labrum (A).	18
13	Coracohumeral ligament and rotator interval.	19
14	Subcoracoid bursa and superior subscapularis recess.	21
15	(a) Demonstrative sagittal view of the shoulder joint. (b) T1 sagittal oblique view of the shoulder. The coraco-acromial ligament	22

Fig.	Title	Page
	(open arrow) anterior to the shoulder is a low	
	signal band between its attachments on the	
1.0	acromion (A) and the coracoid process (C)	22
16	Graphic image of a lateral view of the rotator	23
17	cuff muscle  Coronal image T1 weighted for suppressed	25
1 /	Coronal image T1-weighted fat suppressed MR arthrogram reveals increased signal (white	25
	arrow heads) in the bursal side of the	
	supraspinatus tendon which is due to "Magic	
	angle" artefact	
18	(A) Axial T2-weighted with fat-saturation MR	26
	image of the shoulder showing the normal	
	subscapularis tendon (arrow) and	
	myotendinous junction (arrowhead). Other	
	structures visualized are the deltoid muscle	
	(D), anterior labrum (A), posterior labrum (P),	
	glenoid (G), humeral head (H), and long head	
	of the biceps tendon (L). (B) Coronal-oblique	
	T2-weighted with fat-saturation MR image of	
	the shoulder nicely demonstrates different tendons (arrowheads) arising from the	
	subscapularis muscle	
19	Graphic image of a coronal section A-	27
1,	posterior view B-anterior view of the rotator	
	cuff muscles	
20	Axial T1-weighted MR images of the shoulder	28
	demonstrate (A) an anomalous tendon (white	
	arrow) adjacent and superficial to the long	
	head of the biceps tendon (black arrow) within	
0.1	the bicipital groove.	20
21	Quadrilateral space syndrome.	29
22	MRI anatomy.	30
23	Normal shoulder. Coronal oblique T1	31
24	Normal shoulder. Coronal-oblique T1-	32

Fig.	Title	Page
	weighted MR image shows the normal	
	supraspinatus and infraspinatus muscles and tendons.	
25	MR planes showing how to plane an adequate shoulder MR	33
26	Long head of biceps (LHB) tendon (short axis).	39
27	Long head of biceps (LHB) tendon (long axis).	40
28	Subscapularis tendon (long axis).	41
29	a): Subscapularis tendon (short axis). Transducer placement with shoulder externally rotated Subscapularis tendon (short axis). b): US image shows hyperechoic and	42
20	fibrillar subscapularis tendon (arrows).	42
30	Ultrasound image of the subscapularis tendon with its multipennate appearance showing areas of hyper (white arrows) and hypo echogenicity (asterisk) due to anisotropy as described in the article	42
31	a): Supraspinatus tendon (short axis). Transducer placement with shoulder in modified Crass position (Jacobson, 2011). (b) Corresponding ultrasound image shows hyperechoic supraspinatus (SS) tendon in the short axis. Superficial to the tendon is the hypoechoic subacromial bursa (white arrow) and deep to the tendon on the humeral head (H) is the hypoechoic articular cartilage (white arrowheads). Anterior to the SS tendon is the rotator interval with the long head biceps tendon (B) within it.	45
32	Rotator interval and anterior supraspinatus (short axis). (a) Transducer position with	45

Fig.	Title	Page
8		
	elbow flexed at 90 degrees and pushed	
	posteriorly as far as possible keeping it in the sagittal plane without attempting to put it over	
	the lower back/hip. (b) Corresponding US	
	image shows the rotator interval between the	
	supraspinatus (SS) and subscapularis (Sub)	
	tendons, consisting of the long head of biceps	
	(LHB) tendon (B) and coracohumeral	
	ligament (white arrow) in the roof of the	
	interval and the anterior glenohumeral	
	ligament in its anterior aspect (white star)	
33	a) Supraspinatus tendon (long axis) probe	46
	position (Jacobson, 2011). b) Corresponding	
	ultrasound (US) image shows fibrillar	
	hyperechoic supraspinatus tendon (SS).	
34	Supraspinatus tendon (short axis).	46
35	a) Acromio-clavicular joint. Transducer	48
	placement over superior aspect of the shoulder	
	(b). US image shows acromio-clavicular joint	
	(arrow) with characteristic hyperechoic bony	
	contours of the distal clavicle (C) and	
2.5	acromion (A).	40
36	(a) Dynamic assessment for subacromial	49
	impingement. (a)Transducer placement over	
	superolateral aspect of shoulder in neutral	
27	position. (b) after abduction of the shoulder  Dynamic assessment for subacromial	49
37	Dynamic assessment for subacromial impingement Corresponding US image shows	49
	acromion(A) and greater tuberosity (GT) with	
	supraspinatus tendon (S) and collapsed	
	subacromial-subdeltoid bursa (arrow).	
38	shoulder ultrasound showing correct	49
	measurement of subacromial subdeltoid bursa	
	(1 is a wrong measurement including the	
	(1 is a wrong measurement including the	

Fig.	Title	Page
	peribursal fat ), (2 is the correct measurement	
_	including only the intrabursal fluid)	
39	a) Transducer placement over posterior aspect	51
	of the shoulder in neutral position (Jacobson,	
	<b>2011).</b> b) Transducer position with the	
40	ipsilateral hand on the contralateral shoulder	<i>7</i> 1
40	Corresponding ultrasound image shows the	51
	posterior glenohumeral joint recess (long	
	white arrow) between the humerus (H) and glenoid (G). Long axis view of the	
	infraspinatus muscle (IS) with central	
	hyperechoic myotendinous region and the	
	spinoglenoid notch (short white arrows). L,	
	posterior labrum	
41	Infraspinatus and teres minor (short axis).	52
42	Grade III, moderate acromioclavicular joint	55
	arthritis (ACJ) (encircled) abnormalities	
	demonstrating subacromial fat effacement,	
	joint space narrowing, and irregularity	
43	Acromioclavicular joint, longitudinal view.	55
44	Axial T1-weighted image showing the os	56
45	acromiale	5.0
45	Acromion, transverse view.	56
46	Sagittal oblique T2WI, type I flat acromion (A), type II concave under surface (B) and	57
	type III concave under surface (b) and	
	hook (C)	
47	Coronal fat-suppressed T2-weighted MR	58
	image shows distention of subacromial	
	subdeltoid bursa without rotator cuff tear	
	(arrow)	
48	Coronal sonography view of left shoulder with	59
	subacromial impingement, during active	
	elevation of arm halfway between flexion and	